metals

MDPI

Review

Green Synthesis of Silver Oxide Nanoparticles for Photocatalytic Environmental Remediation and Biomedical Applications

Mir Sayed Shah Danish [1,2,*], Liezel L. Estrella-Pajulas [3,*], Ivy Michelle Alemaida [4], Maria Luisa Grilli [5,*], Alexey Mikhaylov [6] and Tomonobu Senjyu [1]

1 Strategic Research Project Center, University of the Ryukyus, 1 Senbaru, Nishirara 903-0213, Japan; b985542@tec.u-ryukyu.ac.jp
2 Department of Energy Engineering, Kabul University, Jamal Mina, 3rd District, Kabul 1006, Afghanistan
3 Department of Chemistry, Silliman University, Hibbard Avenue, Dumaguete City 6200, Philippines
4 Department of Chemistry, University of San Carlos—Talamban Campus, Cebu City 6000, Philippines; usc.alemaidaim@gmail.com
5 Energy Technologies and Renewable Sources Department, Italian National Agency for New Technologies, Energy and Sustainable Economic Development (ENEA), Casaccia Research Center, 00123 Rome, Italy
6 Financial Research Institute of Ministry of Finance of the Russian Federation, 127006 Moscow, Russia; alexeyfa@yandex.ru
* Correspondence: k208681@eve.u-ryukyu.ac.jp (M.S.S.D.); liezellestrella@su.edu.ph (L.L.E.-P.); marialuisa.grilli@enea.it (M.L.G.)

Abstract: Among the most notable nanotechnology applications is its employment in environmental remediation and biomedical applications. Nonetheless, there is a need for cleaner and sustainable methods in preparing nanomaterials that use cheaper, more environment-friendly precursors than the conventional synthesis process. The green chemistry approach for the preparation of nanoparticles is becoming more attractive as it uses non-toxic chemicals and reagents. It also offers cost-effective synthesis process as it uses readily available plant sources and microbe as redox mediators in converting metallic cations to metal or metal oxide nanoparticles. The extracts of these plants and microbe sources contain phytochemicals and metabolites in variable quantities, which serve as redox mediators and capping agents that stabilize the biosynthesized nanoparticles. The present article reviews the recent studies on the fabrication of silver oxide nanoparticles (Ag_2O-NPs) via plant-mediated and microbe-mediated green synthesis, giving a concise discussion on the green preparation of Ag_2O-NPs employing extracts of different plants and microbial sources. The performances of the biosynthesized Ag_2O-NPs are also reviewed, highlighting their potential use in photocatalysis and biomedical applications.

Keywords: silver oxide nanoparticles; green synthesis; photocatalysis; biomedical applications; metal oxides; photocatalytic degradation

check for updates

Citation: Danish, M.S.S.; Estrella-Pajulas, L.L.; Alemaida, I.M.; Grilli, M.L.; Mikhaylov, A.; Senjyu, T. Green Synthesis of Silver Oxide Nanoparticles for Photocatalytic Environmental Remediation and Biomedical Applications. *Metals* **2022**, *12*, 769. https://doi.org/10.3390/met12050769

Academic Editor: Jürgen Eckert

Received: 22 March 2022
Accepted: 27 April 2022
Published: 29 April 2022

1. Introduction

Nanomaterials behave differently compared to macroscale materials, having highly desirable properties due to size confinement, the dominance of interfacial phenomena due to increased surface area, and quantum effects [1]. These distinctive characteristics of nanosized materials lead to improved performances in catalytic and tunable photo activity, increased strength, etc., making nanomaterials play a major role for a broad range of applications. One of the most notable applications of nanotechnology is its employment in different methods for environmental remediation [2–4]. Industries such as food, pharmacy, cosmetics, paints, plastics, paper, textiles, and even agriculture that use pesticides, release harmful organic pollutants and pathogenic biological pollutants into the environment. Nanotechnology stands at the forefront of today's scientific studies and innovations thanks to its large use in remediation of environmental problems brought by the ever-emerging industrialization and progressive urbanization of today's society [5,6].

Metal oxide nanoparticles have gained particular attention because of their unique physical and chemical characteristics with great potential in environmental remediation. Their applications range from their usage for the removal of heavy metals, poisonous gas sensing, textile, biomedical applications, and photocatalytic degradation of organic contaminants [3,7,8]. Moreover, the emergence of drug-resistant microorganisms created serious problems in treating infections and other diseases. The need to develop different and effective bactericidal agents to deal with drug-resistant bacteria is a challenge [9], and recent studies demonstrated that metal oxide nanoparticles may have great potential in antimicrobial applications. Similarly, metal oxide nanoparticles have been demonstrated as effective in photocatalytic degradation of organic pollutants, especially organic dyes that are among the largest group of hazardous organic compounds causing increased environmental threat and carcinogenic effects [1].

Silver oxide nanoparticles (Ag_2O-NPs) were recently found to have desirable properties for applications in photovoltaic cells, sensors, data storage devices, biomedical applications, and photocatalysis [10,11]. Ag_2O-NPs have been explored in many studies focusing on their synthesis, characterization, and photocatalytic performance. Their good optical properties and narrow bandgap (1.1~1.4 eV), which enables them to absorb the full solar spectrum, make these nanoparticles attractive for visible light driven photocatalytic removal of organic pollutants. Ag_2O-NPs photocatalyst was also reported to undergo self-stabilizing process during photocatalytic degradation of organic compounds, resulting in a high photocatalytic performance [1,12].

In this review paper, we report on the recent studies about Ag_2O-NPs obtained by plant-mediated and microbe-mediated green synthesis. The biomedical and catalytic properties of Ag_2O-NPs prepared by these methods have been discussed.

2. Green Synthesis and Characterization of Ag_2O-NPs

2.1. Green Synthesis

A huge fraction of the nanomaterials being used in many fields nowadays is prepared using chemical and physical methods. Aside from being expensive, conventional synthesis methods are also known to utilize environmentally and biologically hazardous chemicals, such as organic solvents, reducing agents, and stabilizers, thus limiting the use of these nanoparticles in clinical and biomedical fields [1,5]. Hence, many research groups have become interested in developing cost-effective and environmentally safe synthesis processes of nanoparticles that reduce or eliminate the use of hazardous chemicals and avoid the formation of unnecessary and harmful side-products. The green synthesis method of preparing nanoparticles is the best alternative to the existing chemical and physical synthesis methods as it is cheaper, safe to handle, and eco-friendly [13–15].

The fabrication of nanoparticles via the green synthesis method allows the reduction of the metal ions through some supposed metabolic process that requires relatively low activation energy for the synthesis reactions to occur. A considerable amount of research on metal oxides is conducted using microbes and plants, taking advantage of their capabilities to mediate the precursor's redox reactions, forming metal/metal oxide nanoparticles, and stabilizing resulting nanoparticles [15–17]. Bacteria, for example, has been reported to be an effective reducing agent of metal ions. Additionally, bacterial cells are easy to culture, making them convenient for synthesizing any nanomaterial [18]. Fungus has been exploited in the biosynthesis of nanoparticles due to the reductive ability of its proteins and intracellular enzymes [19].

On the other side, the use of plant extracts as reducing agents has also become promising because they contain biomolecules such as carbohydrates, proteins, and coenzymes that possess the capabilities of reducing metal ions. These biomolecules also act as stabilizing and capping agents for the synthesized nanoparticles. Plant-mediated synthesis has the advantage of scalability and speed, with respect to microbe-mediated synthesis. In addition it is inexpensive, readily available and has been proven to be efficient [3,20].

For the above-mentioned reasons, the use of plant sources has become the most attractive and preferred method in the fabrication of nanoparticles.

Figure 1 reports a general scheme of the green synthesis process. Parameters such as temperature, humidity, pH, extract concentration, phytochemical profile, metal ion concentration, and incubation time affect the synthesis process, i.e., nanoparticles goodness, stabilization, quantity produced, and yield rate [21,22].

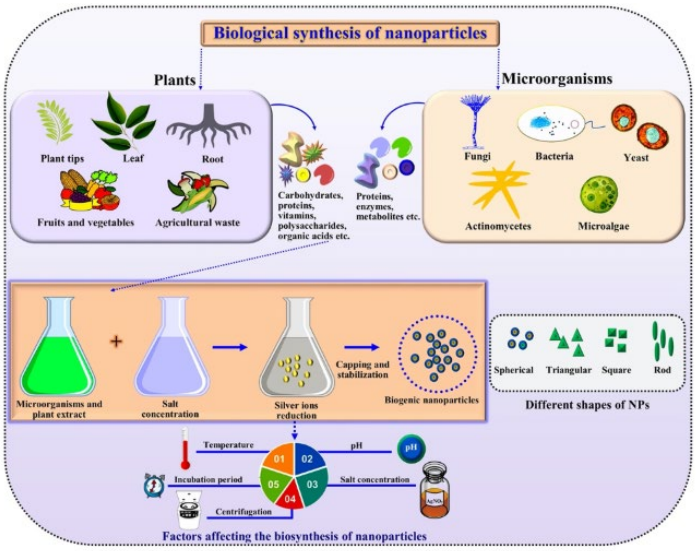

Figure 1. Generalized schematics of green synthesis of nanoparticles. Reprinted from Ref. [22].

2.1.1. Plant-Mediated Synthesis

The use of plant sources for the synthesis of Ag_2O-NPs is by far the most successful green synthesis method. The plant-mediated fabrication of Ag_2O-NPs is reported to be more time-efficient and produces more stable nanoparticles than those prepared using microbe-mediated synthesis [23]. Most importantly, plant sources are readily available, inexpensive, nonhazardous, and contain phytochemicals that can act as stabilizing agents of the resulting nanoparticles [24]. Up to date, the utilization of plant-derived materials continues to progress, as more and more research groups have explored the potential use of different plants for the synthesis of nanoparticles by using extracts of both aerial and underground parts like leaves, roots, stems, fruits, and others [25]. While many studies have reported about plant-mediated biosynthesis of silver nanoparticles (AgNPs) [26,27], the studies presented in this review article report Ag_2O-NPs as the main biosynthesis product instead of AgNPs. While the exact reaction mechanism has not been established yet, Şuţan et al. [28] suggest that some plant extracts contain phytocomponents that are not adequate to act both as reducing agent for Ag^+ to Ag^0 and as a capping agent. This results in the oxidation of AgNPs to Ag_2O-NPs. This finding was supported by the XRD, UV-Vis, and FTIR data. Figure 2 illustrates the proposed reaction mechanism during the formation and stabilization of the Ag_2O-NPs mediated by plant extracts (pentacyclic triterpenoids, asiaticoside, brahmoside, asiatic acid, brahmic acid, flavonoids, moxifloxacin, rhamnocitrin, physcion, kaempferol, maesopsin, quercitin, emodin, etc.) to name some of ingredients of leaves, stem, and roots. The phytochemicals in plants are said to mediate the formation of Ag_2O-NPs, as shown in Equations (1)–(3) [29]. The reaction between the hydroxyl groups (-OH) of the phytochemicals and Ag^+ from $AgNO_3$ initially produces AgOH, which is then converted to Ag_2O [29,30]:

$$AgNO_3 + \text{Phytochemical} \rightarrow AgOH\left(\begin{array}{c}\text{Bonding with}\\ \text{phytochemicals}\end{array}\right) + HNO_3 \quad (1)$$

$$Ag^+ + OH^- \rightarrow AgOH \quad (2)$$

$$2AgOH \rightarrow Ag_2O + H_2O \quad (3)$$

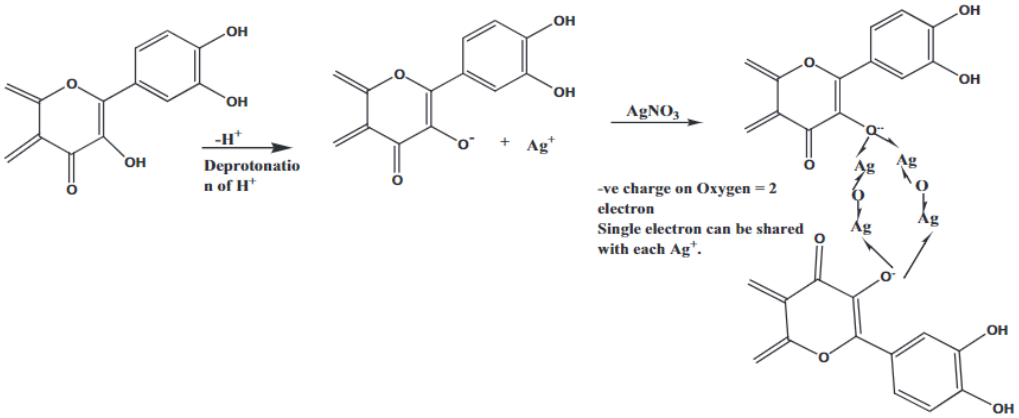

Figure 2. The reaction mechanism during the synthesis of Ag_2O-NPs. Reprinted with permission from Ref. [29] Copyright 2020 Elsevier.

Table 1 lists the summary of the plant-mediated synthesis of Ag_2O-NPs. Among the plant sources currently explored for the synthesis of Ag_2O-NPs, most research reports focus on the use of leaves. Li et al. [24] utilized plant powder of medicinal plant *Lippia citriodora* prepared by drying the leaves in an autoclave and grinding them into a fine powder using a mortar. The plant powder was then mixed with a stoichiometric ratio of silver nitrate ($AgNO_3$) and a minimum amount of water by magnetic stirring. The synthesis reaction took place after heating the mixture in a muffle furnace at 600 °C, producing spherical Ag_2O-NPs with high purity and thermal stability. The obtained nanoparticles resulted in average particle size of 20 nm and were used as photocatalyst and antimicrobial agent. Using a similar method, Rashmi et al. [31] synthesized Ag_2O-NPs, employing finely ground plant powders of *Centella asiatica* and *Tridax procumbens* by mixing them individually with $AgNO_3$. *Centella asiatica*, commonly known as *gotu kola*, belongs to the *Apiacea* family. It is reported to contain pentacyclic triterpenoids, asiaticoside, brahmoside, asiatic acid, and brahmic acid, giving it importance in medicine and cosmetics. *Tridax procumbens*, also known as *Tridax*, belongs to the *Asteraceae* family and contains flavonoids. These compounds have the potential to reduce $AgNO_3$ to Ag_2O as well as to stabilize the resulting nanoparticles. The produced nanoparticles, with a particle size of 11–12 nm, were tested by electrochemical, photocatalysis, and biological studies (Figure 3). Results suggest that the synthesized Ag_2O nanoparticles have excellent electrochemical properties, exhibit good photocatalytic activity for AO-8 under UV light, and also have antimicrobial properties.

Table 1. Plant-mediated synthesis of Ag_2O-NPs.

Plant Source	Particle Size and Shape	Characterization Technique	Applications and Analysis Subject	Ref.
Lippia citriodora (leaf extracts)	20 nm, spherical	XRD, TEM, FTIR, EDX, TGA	Antimicrobial (*Staphylococcus aureus*, *Aspergillus aureus*) photocatalytic activity (Acid orange dye) animal wound healing (Albino mice)	[24]
Centella asiatica and *Tridax procumbens* (leaf extracts)	1112 nm, spherical	XRD, SEM, EDX, FTIR CV, EIS, UV-Vis	Photocatalytic activity (Acid orange dye) Antimicrobial (*Staphylococcus aureus*, *Staphylococcus epidermidis*, *Aspergillus aureus*)	[31]
Helleborus odorus Waldst. and *Kit. Ex Willd* (leaf extracts)	10.45 nm, spherical	UV-Vis, XRD, TEM, EDX	Cytogenotoxicity (Allium assay)	[28]
Trigonella foenum-graecum	30.4 nm, irregular	UV-Vis, FTIR, TEM, SAED	Hemolytic activity (Human blood samples)	[32]

Table 1. *Cont.*

Plant Source	Particle Size and Shape	Characterization Technique	Applications and Analysis Subject	Ref.
Amaranthus sp. (leaf extracts)	81 nm, monodispersed husk	UV-Vis, XRD, SEM, DLS	Photocatalytic activity (caffeine) Antimicrobial (*Escherichia coli*, *Staphylococcus aureus*, *Pseudomonas aeruginosa*)	[33]
Paeonia emodi (leaf extracts)	38.29 nm, mixed phase (cubic and hexagonal)	XRD, SEM, EDX	Photocatalytic activity (Methylene blue) Antimicrobial (*Bacillus subtilis*, *Staphylococcus aureus*, *Escherichia coli*, *Pseudomonas aeruginosa*)	[34]
Pavetta indica Linn. (leaf extracts)	49.8 nm of width 469.2 nm, distorted square	XRD, SEM, EDX	-	[35]
Artocarpus hetrophyllus (leaf extracts)	14 nm, spherical	XRD, UV-Vis, FTIR, DLS, TEM	-	[29]
Artocarpus heterophyllus (rind extract)	17 nm, spherical	UV-Vis, FTIR, TEM, XRD	Antimicrobial (*Phytophthora capsica*, *Phytophthora drechsleri*, *Didymella bryoniae*, *Colletotrichum acutatum*)	[36]
Lawsonia inermis (leaf extracts)	39.1 nm, cubic	XRD, SEM, EDX, FTIR, UV-Vis	Antimicrobial (*Staphylococcus aureus*, *Pseudomonas aeruginosa*, and *Escherichia coli*, *Penicillium* spp., *Candida albicans*, *Aspergillus* spp.)	[37]
Cyathea nilgiriensis (leaf extracts)	<100 nm, mixed phase (hexagonal and spherical)	FTIR, XRD, SEM, EDX	Antimicrobial (*Staphylococcus aureus*, *Bacillus subtilis*, *Micrococcus luteus*, *Escherichia coli*, *Salmonella paratyphi*, *Aspergillus niger*) Anticancer (Cells from tumor bearing mice)	[38]
Daphne alpina (leaf extracts)	38.52 nm, mixed phase (cubic, tetragonal, and hexagonal)	XRD, FTIR, SEM, EDX	Antimicrobial (*Bacillus subtilis*, *Staphylococcus aureus*, *Escherichia coli*, *Pseudomonas aeruginosa*, *Candida albicans*, *Aspergillus niger*)	[39]
Rhamnus virgata (leaf extracts)	20 nm, spherical	EDX, DLS, UV-Vis, FTIR, XRD, Raman, SEM, TEM	Anticancer (HUH-7 and HepG2 cells Cytotoxicity (Brine-shrimps and Leishmanial parasite) enzyme inhibitory (Protein kinase and alpha-amylase) Antibacterial (*Staphylococcus aureus*, *Pseudomonas aeruginosa*, *Bacillus subtilis*, *Klebsiella pneumonia*, *Escherichia coli*) Biocompatibility (Human blood samples)	[40]
Callistemon lanceolatus D.C. (leaf extracts)	330 nm, mixed phase (spherical and hexagonal)	UV-Vis, FTIR, SEM, EDX, XRD, TEM	Antioxidant (total antioxidant activity assay, 2-diphenyl-1-picryl-hydrazyl-hydrate (DPPH) radical scavenging assay, Ferric ion reducing antioxidant power (FRAP) assay, β-carotene bleaching activity assay) Cytotoxicity (Brine shrimp)	[30]
Thunbergia mysorensis (stem and flower extracts)	15 nm and 120 nm, spherical	UV-Vis, FTIR, SEM, TEM, XRD	Antioxidant (DPPH assay, ABTS cation radical, FRAP assay) Hemolytic activity (Human blood samples) Cytotoxicity (Triple-negative breast cancer cell line (TNBC)) Antimicrobial (*Micrococcus luteus*, *Staphylococcus aureus*, *Bacilluscereus*, *Klebsiella pneumonia*, *Escherichia coli*, *Pseudomonas fluorescens*, *Enterobacter aerogenes*, *Salmonella enteritidis*, *Pseudomonas aeruginosa*	[41]
Curcuma zanthorrhiza Roxb. (Rhizome extracts)	17.98–46.73 nm, spherical	UV-Vis, XRD, TEM, TEM, FTIR, HR-LCMS	Photocatalytic activity (Malachite green)	[42]
Zephyranthes Rosea (Flower extracts)	10– 30 nm, spherical	XRD, EDX, TEM, FTIR, SEM, XPS, SAED	Antibacterial (*Escherichia coli*, *streptococcus mutants*, *staphylococcus aureus*) Antioxidant (DPPH assay) Anti-inflammatory (Bovine serum albumin (BSA) assay) Enzyme inhibition (α-amylase)	[43]
Ficus benghalensis (Prop root extract)	42.7 nm, spherical	UV-Vis, FTIR, TEM, SAED, XRD	Antimicrobial (*Streptococcus mutans*, *Lactobacilli* sp.)	[44]

Table 1. *Cont.*

Plant Source	Particle Size and Shape	Characterization Technique	Applications and Analysis Subject	Ref.
Herniaria hirsute (plant extract)	15.51 nm, spherical	UV-Vis, FTIR, XRD, SEM	Photocatalytic activity (Methylene blue)	[45]
Eupatorium odoratum (leaf extract)	23.6 nm, spherical	UV-Vis, XRD, SEM, TEM	Mosquito larvicidal (*Culex quinquefasciatus larvae*) Antimicrobial (*Escherichia coli*, *Salmonella typhi*, *Bacillus subtilis*, *Staphylococcus aureus*, *Candida albicans*)	[20]
Dracaena cinnabari (bark/trunk resin)	20 nm, quasi-spherical	XRD, Raman, FTIR, TEM	Antimicrobial (*Escherichia coli*, *Staphylococcus aureus*)	[46]
Phoenix dactylifera L. (leaf extract)	28–39 nm, mixed phae (oval and spherical)	XRD, SEM, UV-Vis, FTIR	Photocatalytic activity (Congo red, methylene blue)	[47]
Osmium sanctum (leaf extract)	36–40 nm, spherical	SEM, XRD, EDX, TEM, UV-Vis, TGA, FTIR	Photocatalytic activity (Paracetamol)	[48]

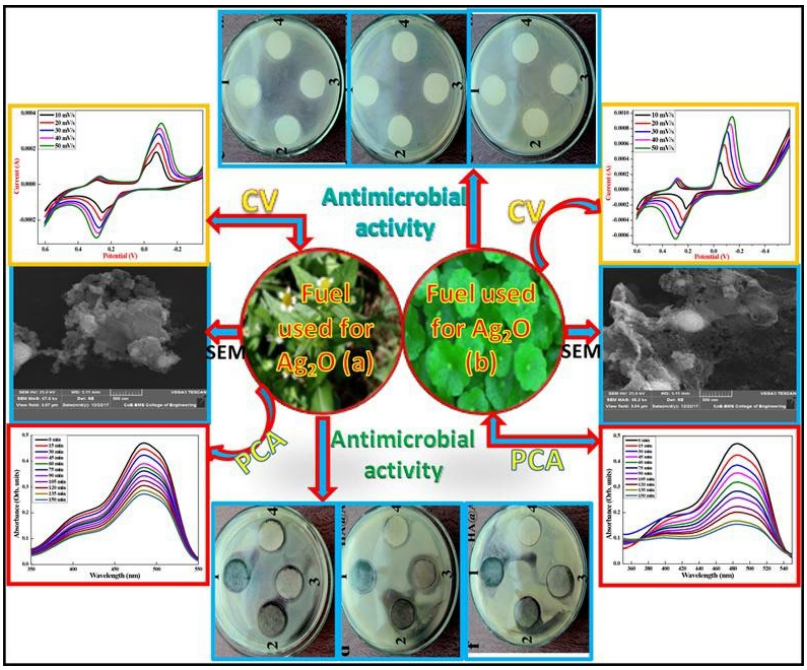

Figure 3. Top: Cyclic Voltammogram and SEM micrographs and of Ag_2O nanoparticles prepared using (**left**) *Centella asiatica* (**right**) *Tridax*. Bottom: Absorbance of Ag_2O-NPs: (**left**) *Centella asiatica* and (**right**) *Tridax* plant extract using AO-8 dye photocatalyst under UV light irradiation. Reprinted with permission from Ref. [31] Copyright 2020 Elsevier.

Şuţan et al. [28] synthesized Ag_2O-NPs through a bottom-up approach using the hydroethanolic leaf extracts of *Helleborus odorus Waldst*. & *Kit. Ex Willd*, a medicinal plant that belongs to *Ranunculaceae* family. The Ag_2O-NPs were synthesized by mixing the crude hydroethanolic leaf extracts with $AgNO_3$ in 1:1 ratio allowing the reaction to occur in the dark at room temperature for 24 h. The obtained nanoparticles were characterized and tested for cytogenotoxic effects. Following a similar procedure, Ashokraja et al. [32] employed leaf extracts of fenugreek (*Trigonella foenum-graecum*) and papaya (*Carica papaya*). The extracts of fenugreek leaves and papaya leaves were separately mixed with $AgNO_3$ and were stirred at room temperature for 8 h, leading to Ag_2O-NPs with particle size range of 19.4–30.4 nm, which were then subjected to hemolytic activity.

Muthukumar et al. [33] reported the synthesis of husk shaped Ag_2O-NPs using leaf extract of *Amaranthus* sp. as reaction mediator and capping agent. To obtain Ag_2O-NPs, aqueous leaf extract of amaranth was slowly added to $AgNO_3$ solution with continuous

magnetic stirring at 35 °C for 20 min. The resulting Ag_2O-NPs were evaluated for potential use as photocatalyst, bactericidal agent, antimicrobial agent, and antioxidant. A similar process was employed by Shah et al. [34] using leaf extracts of *Paeonia emodi* mixed with $AgNO_3$ under continuous stirring at 50 °C for 90 min. The resulting nanoparticles were examined as potential photocatalytic and antimicrobial agent. *Pavetta indica Linn* was used in the synthesis of Ag_2O-NPs as reported by Suresh et al. [35]. Leaf extracts were mixed with $AgNO_3$ solution and continuously stirred at 100–120 °C for 24 h, allowing the formation of distorted cubic shaped nanoparticles with size of 49.8 nm, which were then tested for anti-inflammatory and phytochemical activities.

The biosynthesis of spherical Ag_2O-NPs using *Artocarpus hetrophyllus* plant extract was reported by Archana et al. [29]. *A. hetrophyllus* tree belongs to the *Moraceae* family and is known for the medicinal uses of its leaves, bark, roots and seeds. In the reported study, the aqueous leaf extract was used as a reducing and a capping agent. The Ag_2O-NPs were produced via hydrothermal method by slowly adding the leaf extract to $AgNO_3$ solution in a 1:1 ratio, accompanied by heating and constant stirring at 60–80 °C for 60 min. Using a similar method, Fayyadh et al. [37] employed aqueous leaf extracts of *Lawsonia inermis*, a flowering plant also known as *henna* tree, for the biofabrication of Ag_2O-NPs as antimicrobial agent. Pradheesh et al. [38] employed aqueous leaf extracts of medicinal plant *Cyathea nilgiriensis* and they produced Ag_2O-NPs for antimicrobial and anticancer applications.

The use of *Daphne alpina* in the synthesis of Ag_2O-NPs was reported by Haq et al. [39] and the resulting nanoparticles were functionalized with moxifloxacin, an antibiotic, and used as bactericidal and fungicidal agent. The moxifloxacin-functionalized Ag_2O-NPs were synthesized via sonochemical process by mixing $AgNO_3$ with *Daphne alpina* leaf extract with heating and constant stirring at 50 °C for 60 min. After subsequent centrifugation and drying, the obtained Ag_2O-NPs were dispersed in ethanol and slowly added with moxifloxacin-HCl with continuous stirring for 20 min, followed by sonication of the mixture for 15 min.

Abbasi et al. [40] reported the use of leaf extracts of *Rhamnus virgata* for the biosynthesis of Ag_2O-NPs for potential biomedical applications. *R. virgata* is a common shrub that belongs to *Rhamnaceae* family known to contain a variety of phytochemicals, including herbacetin, rhamnocitrin, physcion, kaempferol, maesopsin, quercitin, and emodin. These phytochemicals make *R. virgata* a medicinally important plant. In the biosynthesis of Ag_2O-NPs, $AgNO_3$ solution was added dropwise to the separate aqueous and ethanolic extracts of *R. virgata.* The prepared nanoparticles were characterized by UV, X-ray diffraction (XRD), Energy Dispersive X-ray Analysis (EDX), Fourier-transform infrared spectroscopy (FT-IR), Dynamic Light Scattering (DLS), Raman, Scanning Electron Microscopy (SEM), and Transmission Electron Microscopy (TEM) to investigate their stability and functionality. NPs were subjected to biological assays including anticancer, cyctotoxicity, alpha amylase, and protein kinase enzyme inhibitory, biocompatibility, antiradical potential, and antimicrobial activity. *Callistemon lanceolatus D.C.* was used for the preparation of Ag_2O-NPs via a novel biosynthesis route as reported by Ravichandran et al. [30]. *C. lanceolatus*, commonly known as a bottle-brush tree belonging to *Myrtaceae* family, is reported to exhibit medicinal properties potentially due the volatile oils, polyphenols, and triterpenoids present in this plant. The Ag_2O-NPs were prepared by mixing the aqueous leaf extracts of *C. lanceolatus* with $AgNO_3$. A small amount of dodecyl sulfate was added as a stabilizing agent for the target nanoparticles. The reaction mixture was placed in a shaking incubator at 37 °C in the dark and the reaction progress was monitored by UV-Vis spectroscopy at regular intervals within 3 h. The nanoparticles were obtained in spherical and hexagonal shapes and were subsequently investigated under cytotoxicity and antioxidant assays.

The use of plant sources not only limits to leaf extracts but also extends to utilization of other plant parts such as stem, roots, and other aerial or underground parts. Kokika et al. [41] reported the use of the stem and flower of *Thunbergia mysorensis* in the synthesis of Ag_2O-NPs in which the flower extracts and stem extracts were separately

employed as mediator and stabilizing agents. This glabrous climber *T. mysorensis*, also known as *kamanabillu balli*, belongs to *Acantaceae* family which has already been explored due to its various uses like antioxidant, cytotoxic, antifungal, and many other potential characteristics. *T. mysorensis* itself is known to possess flavonoids and polyphenols, making it an excellent candidate for the biosynthesis of nanoparticles. Ag_2O-NPs were fabricated by mixing aqueous stem and flower extracts with $AgNO_3$ solution. The mixtures were incubated at 60 °C in the dark with constant stirring for 2–3 h, resulting in the formation of Ag_2O-NPs. Ag_2O-NPs were characterized by SEM, TEM, EDX, and SAE (Figure 4) and used in antimicrobial test, free-radical scavenging activity, cytotoxicity analysis, hemolytic assay, antioxidant activity, and antibacterial assay.

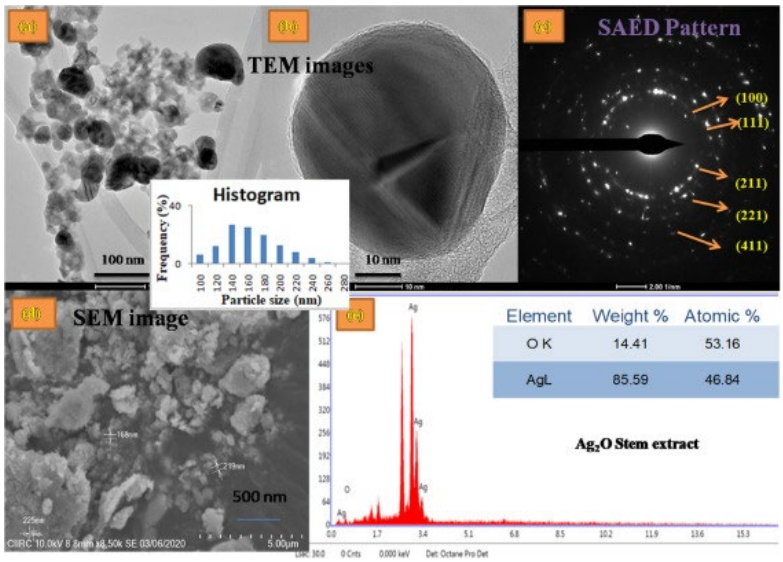

Figure 4. (**a**) TEM image and Histogram, (**b**) Magnified TEM image, (**c**) SAED pattern, (**d**) SEM, (**e**) EDS profile of the Ag_2O–NPs samples prepared using *Thunbergia mysorensis* stem extract. Reprinted with permission from Ref. [41] Copyright 2022 Elsevier.

Aiswariya and Jose [42] reported the successful use of *Curcuma zanthorrhiza* Roxb. *(Cz)* for the synthesis of Ag_2O-NPs. Aqueous rhizome extract of *C. zanthorrhiza* was mixed with $AgNO_3$ followed by sunlight irradiation with continuous stirring for 30 min allowing the formation of Ag_2O-NPs which were then used in the photocatalytic degradation of Malachite green. Analysis revealed that the rhizome extracts contain eleven bioactive molecules, including sesquiterpenoids and lipid molecules acting as reducing and capping agents during the biosynthesis of Ag_2O-NPs.

Maheshwaran et al. [43] prepared face-centered cubic Ag_2O-NPs using the flower extracts of *Zephyranthes Rosea*, a perennial plant belonging to the *Amaryllidaceae* family used to treat several medical conditions such as diabetes, tuberculosis, and breast cancers, among others. The presence of *Amaryllidaceae* alkaloids makes the plant extract a potential agent for the biosynthesis of nanoparticles. The Ag_2O-NPs were synthesized by dropwise addition of the plant extracts to the $AgNO_3$ solution accompanied by constant stirring while keeping the mixture pH within 6.7–11 range by the addition of NaOH solution. The resulting nanoparticles were allowed to precipitate, annealed at 80 °C for 2 h, and then subjected to antibacterial, antioxidant, anti-inflammatory, and anti-diabetic assays.

The preparation of Ag_2O-NPs employing *Ficus benghalensis* prop root extracts as the mediator and capping agent has been reported by Manikandan et al. [44]. *F. benghalensis*, commonly known as Banyan tree, has been used in many medicinal applications and has long been used in relieving toothaches. Authors prepared Ag_2O-NPs by mixing the prop root extracts with $AgNO_3$ solution allowing the mixture to react under constant stirring in ambient condition and the resulting nanoparticles were investigated for bactericidal activity against dental pathogens. In another study reported by Manikandan et al. [36],

Ag_2O-NPs were also successfully fabricated using the rind extracts of *Artocarpus heterophyllus*, the largest tree-borne fruit commonly known as jackfruit and belonging to the *Moraceae* family. The aqueous extract of the jackfruit rind was obtained by boiling finely ground powder of dried jackfruit rind. The Ag_2O-NPs were prepared by mixing the aqueous extracts with $AgNO_3$ solution at ambient temperature. The progress of the reaction was monitored by the color change as well as UV-Vis spectroscopy and the resulting nanoparticles were tested for antifungal activity against plant pathogenic fungi. A similar method was employed by El-Ghmari et al. [45] in utilizing the aqueous extracts of *Herniaria hirsuta* to synthesize Ag_2O-NPs. The nanoparticles were prepared by letting the aqueous plant extracts react with $AgNO_3$ solution under constant stirring for 10 min at room temperature. The resulting nanoparticles were used in photocatalytic degradation of methylene blue dye.

The use of plant sources in the production of metal/metal oxide nanoparticles was also reported. Elemike et al. [20] synthesized heterogeneous silver/silver oxide nanoparticles (Ag/Ag_2O-NPs) using aqueous leaf extracts of *Eupatorium odoratum*, a shrub belonging to the *Asteraceae* family. The oil extract of *E. odoratum* was reported to contain a wide variety of metabolites and phytochemicals, making this plant attractive for medicinal use. A varied ratio of aqueous extracts and $AgNO_3$ solution was mixed under continuous magnetic stirring at 90°C while monitoring the reaction progress by color changes and UV-Vis spectroscopy. This led to Ag_2O-NPs, which were then subjected to antimicrobial and mosquito larvicidal tests. Armani et al. [46] reported on the fabrication of Ag/Ag_2O core/shell and Ag/Ag_2O decorated multi-layered graphene (MLG) nanostructures using a resin obtained from the bark of *Dracaena cinnabari*. This plant, also called dragon's blood, is known to contain bioactive molecules such as flavonoids and tannins, which are potential reducing agents for metal cations and stabilizing agents. To synthesize Ag/Ag_2O-NPs, the aqueous blood red extract, obtained by dissolving the resin powder in water, was added to the $AgNO_3$ solution. The mixture was refluxed with continuous stirring for 1 h and the resulting nanoparticles were allowed to precipitate. Following the same procedure, the Ag/Ag_2O decorated MLG was synthesized by mixing MLG-ethanol suspension with $AgNO_3$ solution. Laouini et al. [47] prepared Ag/Ag_2O-NPs by mixing aqueous leaf extracts of *Phoenix dactylifera* L. with $AgNO_3$ solution and the resulting nanoparticles were used for the photocatalytic degradation of congo red and methylene blue dyes. Zia and Riaz [48] utilized *Osmium sanctum*, also known as holy basil, in the synthesis of polythiophene-sensitized Ag/Ag_2O-NPs heterogeneous photocatalyst. The ethanol: water (50% *v*/*v*) leaf extract was added to $AgNO_3$ solution and the mixture was subjected to microwave irradiation for 5 min. The Ag/Ag_2O-NPs were obtained after centrifugation and subsequent washing with appropriate solvent and calcination at 600 °C. The produced nanoparticles were tested for photocatalytic activity.

2.1.2. Microbe-Mediated Synthesis

Microbial sources are also employed in the green synthesis of many important metal and metal oxide nanomaterials. This includes the use of algae, fungi, bacteria, viruses, and yeast, mainly taking advantage of the proteins and intracellular enzymes present in these microbes. In addition, these green synthesis mediators are environment-friendly, readily available, cost-effective, and easy-to-handle [16,49–51]. To date, reported studies on microbe-mediated synthesis of Ag_2O-NPs have utilized bacteria, cyanobacteria, and fungus, as listed in Table 2.

Dhoondia et al. [52] reported the biosynthesis of Ag_2O-NPs mediated by *Lactobacillus mindensis* isolated from fixer solution. Ag_2O-NPs were prepared by adding the wet biomass obtained from the inoculated *Lactobacillus* sp. to $AgNO_3$ solution. The reaction progress was monitored for color changes along with UV-Vis spectroscopy while keeping the solution at pH 8. The resulting nanoparticles were found to have an average size of 32.5 nm at variable shapes, with a dominant spherical form (Figure 5). The selected area electron diffraction pattern (Figure 5f) confirms the plane (111) of silver oxide. For the exact mechanism for the biosynthesis of Ag_2O from Ag^+, the authors proposed the aldehydic groups present in the

polysaccharides secreted by *Lactobacillus* sp. acted in the bioreduction of Ag^+ to Ag^0 and the subsequent production of Ag_2O-NP. The synthesis of Ag_2O-NPs using *Bacillus thuringiensis* SSV1 culture supernatant was reported by Karunagaran et al. [53]. The nanoparticles were prepared by mixing the supernatant culture and $AgNO_3$ solution. The pH of the solution was adjusted to pH 9 and the solution was in incubation at 80 °C while monitoring the color change throughout the reaction. The obtained nanoparticles were spherical in shape with an average size of 30 nm. These nanoparticles were tested for potential cytotoxic activities. Dharmaraj et al. [18] successfully utilized *Bacillus paramycoides* in the synthesis of Ag_2O-NPs for antibacterial and cytotoxicity applications. The Ag_2O-NPs were prepared mixing the supernatant culture of *bacillus paramycoides*, isolated from mangrove sediment, with $AgNO_3$ solution with the reaction temperature kept at 35 °C while monitoring color changes as an indication of the reaction progress. The products were obtained as spherical nanoparticles with diameter within 25–70 nm range.

Table 2. Microbe-mediated synthesis of Ag_2O-NPs.

Microbial Source	Particle Size and Shape	Characterization Technique	Applications and Analysis Subject	Ref.
Lactobacillus mindensis	32.5 nm, spherical	UV-Vis, TEM, XRD	-	[52]
Bacillus thuringiensis SSV1	30 nm, spherical	XRD, FTIR, EDX, SEM	• Cytotoxicity – HepG2 and Chang liver cell lines	[53]
Bacillus paramycoides	25–70 nm, spherical	UV-Vis, XRD, FTIR, HRTEM	• Antimicrobial – *Vibrio parahaemolyticus*, *Salmonella* sp., *Enterobacter* sp., *Micrococcus* sp. • Cytotoxicity – A549 Lung cancer cells	[18]
Oscillatoria sp.	14.42–48.97 nm, quasi-spherical	UV-Vis, TEM, XRD, FTIR	• Cytotoxicity – CaCo-2, HeLa, and WISH cell lines	[54]
Chlorella vulgaris	85 nm	SEM, EDX, UV-Vis	-	[55]

The use of cyanobacteria in the sustainable preparation of Ag_2O-NPs was reported. El-Sheekh et al. [54] employed *Oscillatoria* sp. to synthesize Ag_2O-NPs by mixing the microalgal biomass with $AgNO_3$ solution and incubating for 24 h. The obtained nanoparticles, quasi-spherical in shape with 14.42–48.97 nm diameter, were assessed as anticancer agents. Green microalgae *Chlorella vulgaris* was used by Yildirim et al. [55] in the fabrication of Ag_2O-NPs for biological hydrogen production. Nanomaterials with particle size of 85 nm were produced by mixing the aqueous microalgae extracts with $AgNO_3$ solution and heating the mixture to 60 °C in the dark.

Heterogeneous nanomaterial Ag/Ag_2O-NPs were also prepared using microbe-mediated green synthesis. Islam et al. [19] reported the successful biofabrication of water-dispersible mycogenic Ag/Ag_2O-NPs using endophytic fungus *Fusarium oxysporum*. The nanoparticles were prepared by mixing fungal mycelia with Ag_2O micro powder under shaking conditions with pH 7 at 25 °C. Changes in color of the mixture monitored the reaction progress. The nanoparticles were obtained as spherical, with particle size ranging between 5–10 nm. The prepared nanoparticles were evaluated for electrochemical glucose sensing, antibacterial, antifungal, and photocatalytic activity.

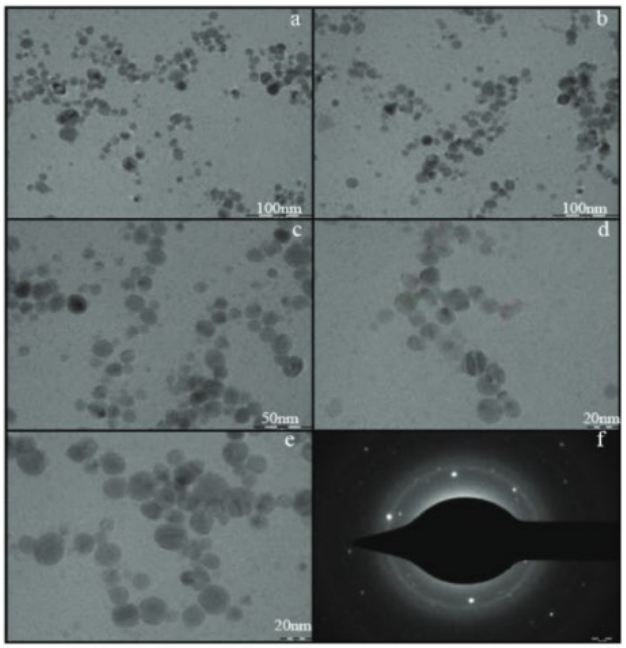

Figure 5. TEM images of silver oxide nanoparticles synthesized by *Lactobacillus mindensis* (low resolution images (**a**–**c**) and high resolution images (**d**,**e**). Selected area electron diffraction pattern (**f**)). Reprinted from Ref. [52].

2.2. Characterization Techniques

To date, plant-mediated and microbe-mediated sustainable green synthesis methods for the preparation of Ag_2O-NPs are gaining popularity for diverse industrial and biomedical applications such as bioimaging, drug delivery, photocatalysis, antimicrobial, and cyctotoxity properties, among others. The nanomaterial's potential in these fields can be assessed by evaluating the intrinsic properties of the nanoparticles determined by the optical activity, surface chemistry, particle size, morphology, crystallinity, structure, and composition [52].

UV-Vis absorption spectroscopy is employed in the determination of the optical absorption and bandgap of the nanoparticles. This technique is used to identify and characterize metal-based nanomaterials based on their absorption. Additionally, knowing the optical band gap is crucial in assessing the photocatalytic potential of the nanomaterial [1,7]. Vital information about the surface chemistry of the nanoparticles can be obtained by employing FTIR. Using this technique, functional groups present on the surface of the nanoparticles can be identified. Therefore, the role of phytochemicals and metabolites on stabilizing the biosynthesized nanoparticles can be understood [33]. This also helps in the interpretation of the activity of the nanoparticles such as antimicrobial activity where surface phytochemicals play a potential role. The bioactive molecules bound on the nanoparticle can be further confirmed using high resolution liquid chromatography mass spectroscopy (HR-LCMS) [42]. Transmission electron microscopy and scanning electron microscopy are used in obtaining information regarding the particle size, purity, internal structure, and morphology of the nanoparticles [24]. The particle size and hydrodynamic size distribution can be examined by employing DLS [7]. This technique is also used in investigating the stability of the nanoparticles. The nanoparticles' lattice dimension, structure, and crystallinity can be determined using XRD. Every crystalline solid possesses unique atomic structure, which shows characteristics of the XRD pattern [33]. In addition, the crystal lattice plane can also be examined from the selected area electron diffraction pattern obtained from high-resolution TEM [32]. Energy dispersive X-ray analysis (EDX or EDAX) is employed for elemental analysis of the composition of the nanomaterial [7,24,56]. The purity of the metal oxide can be determined using X-ray photoelectron spectroscopy (XPS) by examining the chemical states and the binding energy peaks of the compound. The absence of unexpected peaks

indicates purity of the metal oxide. Furthermore, the thermal stability of the nanomaterial can be determined by thermogravimetric analysis (TGA) [48].

The formation of Ag_2O-NPs can be confirmed by the UV-Vis spectrum which exhibits a distinct peak in the range from 420 nm to 440 nm due to the surface plasmon resonance of Ag_2O-NPs [18,32,33,41]. The XRD spectrum of the biosynthesized Ag_2O-NPs exhibits distinct peaks corresponding to the (110), (111), 200), (211), (222), and (311) crystallographic planes which are consistent with the standard data for Ag_2O-NPs (JPCDS No. 76-1393) [28,30,40,41,43]. The formation of Ag–O bond can be further confirmed by the presence of peaks between 450 cm^{-1} and 500 cm^{-1} in the FTIR spectrum [17,21,28]. The excellent thermal stability of biosynthesized NPs was reported by Zia and Riaz [48] using TGA by which thermal decomposition of Ag_2O to Ag was recorded at 805 °C.

3. Photocatalytic Activity of Ag_2O-NP

Ag_2O-NPs are among the promising, efficient, and cost-effective metal oxides used as a photocatalyst for sustainable environmental remediation [37]. The narrow bandgap, 1.46 eV, makes silver oxide nanoparticles a suitable photocatalyst for the degradation of organic dyes under visible light radiation [10,11]. This section reports the photocatalysis mechanism using Ag_2O-NPs and the recent progress in the development and applications of Ag_2O-NPs via green synthesis for such application.

3.1. Mechanism

The high stability of Ag_2O-NPs is one of their interesting attributes, resulting in high photocatalytic activity. Wang et al. reported that during photocatalysis of organic substances, there is a partial formation of metallic Ag on the surface of the Ag_2O, which aids in maintaining the stability of the nanophotocatalyst. The metallic Ag also participates in the photodegradation of the organic pollutants, thus making the photocatalysis process more efficient [12]. The photocatalysis mechanism and the self-stabilization process of Ag_2O-NPs during photocatalysis are shown in Figure 6 and described by Equations (4)–(12) [1,12].

$$Ag_2O + \ h\nu \rightarrow \ Ag_2O\ (e^-_{CB} \ + h^+_{VB}\ ) \quad (4)$$

$$Ag_2O + \ h\nu \rightarrow \ Ag_2O\ (e^-_{CB} \ + h^+_{VB}\ ) \quad (5)$$

$$Ag_2O + e^-_{CB} \ \rightarrow Ag^+ + \ O_2^- \ (\text{electron transfer}) \quad (6)$$

$$Ag^+ + e^-_{CB} \ \rightarrow Ag \ (\text{electron trapping}) \quad (7)$$

$$O_2 + \ e^-_{CB} \ + 2H^+ \rightarrow \ H_2O_2 \quad (8)$$

$$H_2O_2 + \ e^-_{CB} \ \rightarrow \ OH^- + \bullet OH \quad (9)$$

$$H_2O \ + \ h^+_{VB} \ \rightarrow \ H^+ + \bullet OH \quad (10)$$

$$Dye + \bullet OH \rightarrow degradation\ products \quad (11)$$

$$Dye + h^+_{VB} \ \rightarrow oxidation\ products \quad (12)$$

Upon irradiation, the Ag_2O-NPs photocatalyst absorbs photon resulting in the formation of electron–hole pair (Equation (4)) by which the electron (e^-) moves to the conduction band (CB), and the hole (h^+) moves to the valence band (VB). Since Ag_2O has a more negative potential (0.2 V vs. NHE) than Ag^+/Ag (0.7991 V vs. NHE) but is more positive compared to the O_2/H_2O (−0.046 V vs. SHE), the Ag^+ lattice captures the photogenerated electrons (Equation (6)) from the CB of the Ag_2O-NP. The reduction of Ag^+ results in the formation of the metallic Ag on the surface of the Ag_2O. These metallic Ag clusters formed on the photocatalyst surface serve as an electron pool during the multistep photocatalysis. When some amount of metallic Ag has been accumulated, the following photogenerated electrons are expected to transfer to the metallic Ag sites subsequently captured by O_2 dissolved in solution in a multielectron-transfer route (Equations (7) and (8)). The removal of the organic pollutant, such as organic dyes, happens when the generated hydrogen

peroxide captures an electron, and the holes in the valence band are captured by the surface water molecule creating the reactive hydroxyl radical species that subsequently attack the organic substance (Equations (9)–(11)). Moreover, the direct capture of the organic molecule's photoinduced holes also results in the direct oxidation of the target organic pollutant (Equation (12)) [1,11,12,31].

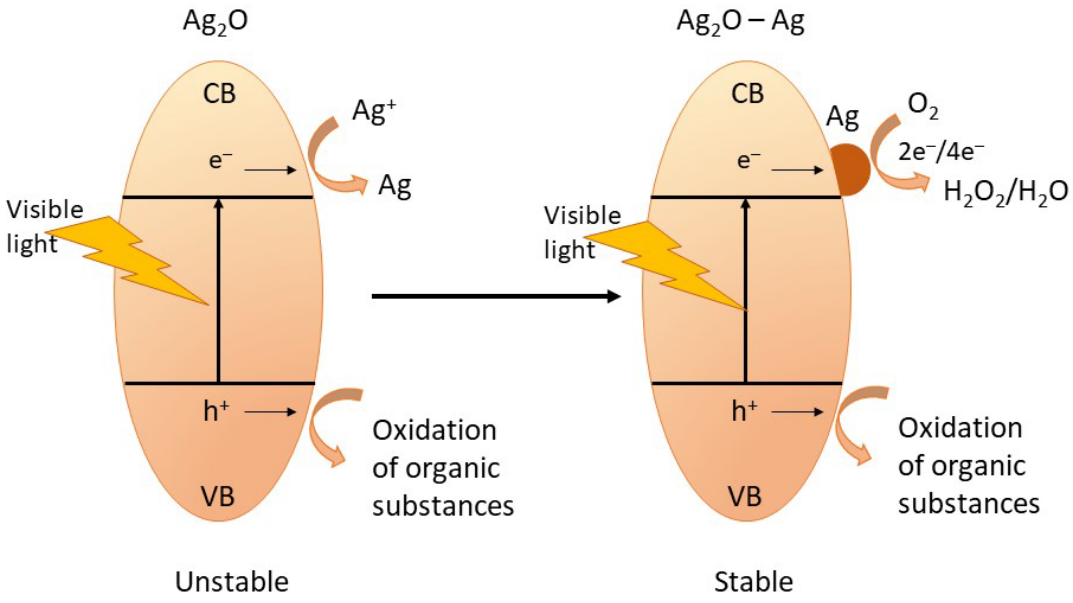

Figure 6. The schematic diagram showing the self-stabilizing process of Ag_2O-NPs during photocatalysis. Adapted from Ref. [12], Copyright 2011 Wiley.

3.2. Photocatalytic Degradation of Organic Pollutants

The biofabrication and development of Ag_2O-NPs photocatalysts via green synthesis has now gained valuable research attention and promising applications for the photodegradation of organic pollutants. Li et al. [24] reported the preparation of Ag_2O-NPs from the plant powders of *Lippta citriodora* via green combustion synthesis. The photocatalytic potential of the obtained Ag_2O-NPs was examined against acid orange 8 (AO8) dye as a target organic pollutant under UV light irradiation, displaying over 40% degradation of the dye over 150 min. As already mentioned previously, a similar green combustion method was used by Rashmi et al. [31] to synthesize Ag_2O-NPs from medicinal plants *Centella asiatica* and *Tridax plant* powders. The photocatalytic activity of the nanoparticles prepared from both plants exhibited potentially high degradation of the AO8 dye. Interestingly, the nanoparticles prepared from *Tridax* recorded 70% photocatalytic degradation which is higher than that of the NPs prepared from *Centella Asiatica* (40%) under 140 min of UV irradiation. The potential of Ag_2O-NPs in the degradation of caffeine, was recently reported by Muthukumar et al. [33]. The Ag_2O-NPs were prepared using green amaranth leaf extract. A notable photocatalytic degradation of 99% of caffeine was observed after 15 h of irradiation with compact fluorescent lamp illumination. These results offer cost-effective and eco-friendly method of removing caffeine as a water pollutant whose elimination using conventional treatment was found rather difficult [57]. El-Ghamari et al. [45] synthesized 15.51 nm Ag_2O-NPs using the extracts of *Herniaria hirsute* (*H. hirsute*) wild plant. When used as a photocatalyst to degrade the target pollutant methylene blue dye in solution in the presence of $NaBH_4$ reducing agent, an 88.6% photodegradation was observed only within 35 min of white light irradiation at room temperature. The same target pollutant was used in the study reported by Shah et al. [34] wherein Ag_2O-NPs synthesized using *Paeonia emodi* showed 97.78% degradation of methylene blue after 3 h of irradiation. Green-synthesized Ag_2O-NPs are also an effective photocatalyst for the degradation of the toxic Malachite green dye, as reported by Aiswariya and Jose [42]. As already mentioned,

in their study, Ag_2O-NPs were prepared using the aqueous rhizome extract of *Curcuma zanthorriza Roxb. (Cz)* and the obtained nanoparticles were used to degrade the Malachite green dye under sunlight and UV light irradiation for 4 h and 24 h, respectively. Interestingly, the decolorization of the Malachite green solution treated with Ag_2O-NPs was more rapid under sunlight irradiation resulting in 94.7% degradation within 4 h, while only 22.83% degradation was recorded under UV irradiation. Further characterization of the photodegradation by-products revealed the absence of toxic chemical entities after the degradation process.

Ag/Ag_2O-NPs heterogeneous photocatalysts prepared using green synthesis were reported efficient in the photocatalytic removal of organic pollutants. Laouini et al. [47] reported Ag/Ag_2O-NPs biosynthesis using leaf extracts of *Pheonix dactylifera* L. as a reaction mediator, giving nanoparticles with size ranging from 28 to 29 nm. The photocatalytic activity of the nanoparticles was examined against Congo red and Methylene blue dyes. An 80% photodegradation of Congo red was recorded after 60 min of irradiation, while 84.5% of the Methylene blue dye in the presence of $NaBH_4$ was photodegraded after 50 min. Zia and Ruiz [48] used *Osmium sanctum* plant extract to biofabricate crystalline Ag/Ag_2O-NPs with sizes ranging between 36 and 40 nm. The photocatalytic potential of the prepared heterogeneous Ag/Ag_2O-NPs was examined against paracetamol drug in which 46% degradation was recorded after 20 min of microwave irradiation. When the heterogeneous photocatalyst was sensitized with polythiophene (PTh) a notable 80% of the paracetamol was degraded after 20 min, implying the enhancement of the Ag/Ag_2O-NPs due to the PTh. A recent study published by Islam et al. [19] reports the biosynthesis of a highly stable, water-dispersible mycogenic Ag/Ag_2O-NPs using the endophytic fungus *Fusarium oxysporum* via a top-down approach. When used for catalytic degradation against Methylene blue dye in the presence of $NaBH_4$, a photodegradation of 86.5% was recorded, notably higher in comparison to the Ag_2O micro powder control photocatalyst, which only showed 50.6% photodegradation.

4. Biomedical Applications of Ag_2O-NPs

4.1. Antimicrobial Effects

One of the main problems today is the antibiotic resistance of bacteria, which makes the treatment of infectious diseases increasingly difficult. Recently, nanomaterials have emerged as new antibacterial agents and their properties as antibacterial and antifungal agents are now of great interest and therefore intensively investigated. Ag_2O-NPs penetrating the bacteria is thought to interact highly with molecules with sulfur and phosphorus groups like DNA. The DNA then loses its ability to replicate, halting the cell cycle at the G2 phase (phase directly preceding mitosis) because of the damage [9]. The nanoparticles induce the generation of reactive oxygen species (ROS) that leads to apoptosis or cell death [58,59]. Another notion for the bactericidal effects of the Ag_2O-NPs is the release of silver ions after penetration [9,60]. The release of atomic Ag^0 and ionic Ag^+ clusters causes cell death following inhibition of a respiratory enzyme by these clusters, resulting in the production of reactive oxygen species such as hydrogen peroxide and the other free radicals, thereby rendering bacterial enzymes inactive [61].

The biosynthesis using plant extracts has been favorably employed compared to other synthesis techniques because of their availability and presence of various phytochemicals that act as reaction mediators and capping agents for the production of nanoparticles. Some plants also already display antimicrobial activities that may be beneficial to the production of nanoparticles requiring antimicrobial properties. Moreover, Ag_2O-NPs prepared using plant-based green method showed increased antimicrobial activity due to the presence of the bioactive functional groups adsorbed on the surface of the nanoparticles [40]. Ag_2O-NPs have been synthesized from *Ficus benghalensis* prop root extract, and its antibacterial activity against the dental bacterial strains *Streptococcus mutans* and *Lactobacillus acidophilus* was assessed [44]. It was shown that a blend of the plant extract plus the produced Ag_2O-NPs showed high antibacterial activity greater than commercial silver nanoparticles

(AgNPs) and it was suggested that the blend can be useful for the production of toothpaste. Furthermore, the biosynthesis of Ag_2O-NPs using the extracts of *Centella asiatica* and *Tridax* has been studied to show antibacterial activities against *Staphylococcus epidermidis* and *Staphylococcus aureus* and antifungal activities against *Aspergillus fumigates* and *Aspergillus aureus* [31]. Ag_2O-NPs synthesized using the leaf extracts of *Rhamnus virgata* also exhibited bactericidal potential against *Staphylococcus aureus*, *Pseudomonas aeruginosa*, *Bacillus subtilis*, *Klebsiella pneumonia*, and *Escherichia coli*. Antifungal activity was also observed against *Aspergillus flavus*, *Fusarium solani*, *Aspergillus niger*, *Candida albicans*, and *Mucor racemosus*. Among the targets, the maximum antimicrobial potential was recorded against *Bacillus subtilis*, *Escherichia coli*, *Mucor racemosus*, and *Aspergillus niger* [40]. Ag_2O-NPs produced from the flowers of *Zephyranthes Rosea* also showed potential antimicrobial activities against the bacteria *Escherichia coli*, *Staphylococcus aureus* and *Streptococcus mutants* [43]. Ag_2O-NPs prepared using the leaf extracts of *Cyathea nilgiriensis* also showed antimicrobial activity against *Staphylococcus aureus*, *Bacillus subtilis*, *Micrococcu luteus*, *Escherichia coli*, *Salmonella paratyphi*, *Klebsiella pneumoniae*, *Candida albicans*, and *Aspergillus niger* [38]. Biosynthesized Ag/Ag_2O-NPs using the extract of *Eupatorium odoratum* leaves showed antimicrobial activity against the *Escherichia coli*, and *Salmonella typhi*, *Bacillus subtilis*, *Staphylococcus aureus*, and *Candida albicans* [20]. Ag_2O-NPs biosynthesized using *Lippia citriodora* extract also showed antimicrobial activity against *Staphylococcus aureus* and antifungal effects against *Aspergillus aureus* [24]. The antimicrobial effects of Ag_2O-NPs have also been employed into fabrics [61–63]. A suspension of Ag_2O-NPs in chitosan solution was incorporated into a cotton fabric and its antimicrobial activity has been found to be effective against *Staphylococcus aureus* and *Escherichia coli* at pH 5 and 7 [62].

Antimicrobial activities of biosynthesized Ag_2O-NPs using fungus were also reported. Ag_2O-NPs prepared using the supernatant culture of *Bacillus paramycoides* showed antibacterial properties against marine biofilm forming bacteria *Vibrio parahaemolyticus*, *Salmonella* sp., *Enterobacter* sp., and *Micrococcus* sp. The FTIR analysis on these nanoparticles confirmed the presence of the metabolite functional groups, which aid in the antibacterial activity. The study reported that treating the bacterial cell with Ag_2O-NPs damages the cell membrane, forcing the release of intracellular constituents and thereby resulting in bacterial cell death [18]. These antimicrobial studies show the great potential of Ag_2O-NPs for various applications in the biomedical field.

4.2. Cytotoxicity

Ag_2O-NPs have shown antioxidant and cytotoxic properties in several studies. A study reporting the biosynthesis of Ag_2O-NPs using *Bacillus paramycoides* showed significant cytotoxicity on A549 lung cancer cells, with IC_{50} values as 58.5 μg mL^{-1}, showing signs of apoptosis as observed under fluorescent microscope [18]. As was mentioned above, it is hypothesized that the nanoparticles induce apoptosis through generation of reactive oxygen species as found by Hsin et al. [58]. These cytotoxicity studies show that Ag_2O-NPs show promise as an anticancer agent. The anticancer properties of Ag_2O-NPs were evaluated by Iqbal et al. [56], confirming the characteristics of biointeraction and physicochemical properties as an anticancer agent of the Ag_2O-NPs. At 60 μg mL^{-1} Ag_2O-NPs concentration, 70% cell viability loss was recorded for HepG2. Analysis on reactive oxygen species revealed that cell death is caused by oxidative stress. Furthermore, the study showed the benefit of keeping these anticancer characteristics at a localized required site. Another study on biosynthesis of Ag_2O-NPs using *Callistemon lanceolatus* extract also showed high cytotoxic activity against brine shrimp nauplii in various in vitro applications, further showing potential for biomedical applications [30]. The biosynthesis of silver oxide nanoparticles using *Cyathea nilgiriensis Holttum* also showed significant anticancer properties. The in vitro cytotoxicity of the Ag_2O-NPs was evaluated using Trypan blue dye assay method. The silver oxide nanoparticles were found to have effective cytotoxic effects, especially increasing concentrations from 10 to 200 μg mL^{-1} [38].

Abbasi et al. [40] reported that the Ag_2O-NPs synthesized using the leaf extracts of *Rhamnus virgata* exhibited strong anticancer activity against HUH-7 and HepG2 cell lines. At a concentration of 900 μg mL^{-1}, the Ag_2O-NPs synthesized from aqueous extracts showed 79% and 83% mortality against HUH-7 and HepG2 cells, respectively. On the other hand, 77.56% and 78.31% mortality against HUH-7 and HepG2 cells, respectively, were recorded using the same concentration of the nanoparticles prepared from ethanolic extracts. These nanoparticles also showed potential cytotoxicity against Leishmanial parasite and brine shrimp. In another study, the Ag_2O-NPs prepared using *Callistemon lanceatus D.C.* also showed cytotoxicity against brine shrimp [30]. In addition, the Ag/Ag_2O-NPs synthesized using *Eupatorium odoratum* exhibited high larvicidal activity against III and IV instar larvae of *Culex quinquefasciatus* noting its great potential for biological application to reduce problems associated with mosquitoes and other insects [20]. Potential antitumor property of Ag_2O-NPs prepared using leaf extracts of *Helleborus odorus Waldst.* and *Kit. Ex Willd* was reported. Cytogenotoxicity test using Allium assay showed the mitodepressive action of the Ag_2O-NPs. Cytological aberration was also observed, which could be caused by the penetration of the nanoparticles on the cell membrane, resulting in membrane disruption and eventually cell death [28].

4.3. Antioxidant Activity, Enzyme Inhibition, Anti-Inflammatory, and Wound Healing Property

The antioxidant properties of the biosynthesized Ag_2O-NPs were also reported. In separate studies, Ravichandran et al. [30] and Kokila et al. [41] investigated the antioxidant property of biosynthesized Ag_2O-NPs. The findings from the various antioxidant assays, including 2,2-diphenyl-1-picryl-hydrazyl-hydrate (DPPH) radical scavenging activity, 2,2′-azinobis-(3-ethylbenzothiazoline-6-sulfonicacid) (ABTS) decolorization, and ferric ion reducing antioxidant power (FRAP) assays, showcased the significant antioxidant potential of the biosynthesized Ag_2O-NPs. The observed antioxidant activity could be attributed to the phytochemicals like flavonoids and other phenolic molecules which serve as the capping agents of the metal oxide.

The wound healing effects and anti-inflammatory properties of metal oxides were also investigated. In a study reported by Gouda [63], gauze fabrics treated with Ag_2O-NPs were tested on rabbit skin and showed substantial wound healing properties, showing a noteworthy effect on granulation tissue formation, infiltrating cells, and a minor effect on the degree of re-epithelialization. This wound healing activity of the Ag_2O-NPs was also shown by Li et al. [24]. A hydrogel was developed using Ag_2O-NPs biosynthesized using *Lippia citriodora* extract and treated to albino mice and showed accelerated wound healing effects. Maheshwaran et al. [43] reported the anti-inflammatory effects of Ag_2O-NPs synthesized from *Zephyranthes Rosea*. When used in Bovine serum albumin (BSA) technique, the prepared Ag_2O-NPs showed significant inhibition of the denaturation process of the albumin, resulting in 97.19% inhibition at a nanoparticle concentration of 500 μg/mL.

Enzyme inhibition is among the potential application of biosynthesized Ag_2O-NPs. In a study conducted by Abassi et al. [40], already mentioned, Ag_2O-NPs were used as antidiabetic agents by investigating their potential in the inhibition of α-amylase, the enzyme responsible for the conversion of carbohydrates to glucose. The Ag_2O-NPs prepared using aqueous and ethanolic extracts of *R. Virgata* showed α-amylase inhibition of 25% and 23%, respectively, at 900 μg/mL nanoparticle concentration. In a separate study using Ag_2O-NPs prepared using *Zephyranthes Rosea* flower extract, an α-amylase inhibition activity of 75.7% was observed at a nanoparticle concentration of 500 μg/mL [43].

4.4. Hemolytic Activity and Biocompatibility

Since some of the biomedical applications of metal oxides involves direct blood contact, the blood compatibility of the metal oxide nanoparticle must be scrutinized in order to ensure biocompatibility and biosafety. The small size and high surface of nanomaterial may meddle with their hemolytic activity. When exposed to the bloodstream, the nanomaterial may cause the red blood corpuscles (RBCs) to lysis and release the hemoglobin, relating

to health ailments. Kokila et al. [41] scrutinized the biocompatibility of biosynthesized Ag_2O-NPs using the flower and stem extracts of *Thunbergia mysorensis*. Apparently the Ag_2O-NPs produced from the flower and stem extracts showed hemolysis activity of 1.0% and 1.4%, respectively. With hemolysis activity values lower than 2–5%, the biosynthesized nanoparticles are considered safe and non-hemolytic. Nonetheless, it is important to stress that the bio effects caused by Ag_2O-NPs could be dependent on concentration and nanoparticle size as well as blood pH [32,41]. The concentration-dependent hemolytic activity of Ag_2O-NPs prepared using *Rhamnus virgata* extracts was also reported, confirming that the *Rhamnus virgata*-mediated Ag_2O-NPs are not hemolytic at low concentrations against RBCs. These findings conclude the biocompatibility of the biosynthesized Ag_2O-NPs [40].

5. Conclusions

Green synthesis is by far the best sustainable method for the preparation of nanoparticles, employing plant sources and microbes as redox mediators in converting metallic cations to metal/metal oxide nanoparticles. Extracts from the plant sources and microbe contain variable phytochemicals and metabolites, which can also serve as capping agents that stabilize the biosynthesized nanoparticles.

The advantages with respect to traditional synthetic approaches are low costs, safety, and eco-friendliness, thus justifying the increasing interest which green synthesis gained in the last decades.

In this review, many studies on the fabrication of Ag_2O-NPs via plant-mediated and microbe-mediated green synthesis found in the recent literature are reviewed and discussed. Several plant sources have been considered such as *Lippia citriodora*, *Tridax procumbens*, *Centella asiatica*, *Carica papaya*, *Curcuma zanthorrhiza*, *Helleborus odorus*, *Trigonella foenum-graecum*, *Amaranthus* sp., *Paeonia emodi*, *Pavetta indica*, *Daphne alpina*, *Rhamnus virgata*, to name only a few. Many of them are also medicinal plants already known for their therapeutic uses. On the other hand, several microbial sources, including bacteria, cyanobacteria, and fungus, have been considered as well. The synthetic approaches employing extracts of plants and microbial sources have been briefly discussed, together with the characterizations and performances of the biosynthesized Ag_2O-NPs, highlighting their potential in photocatalysis and biomedical applications.

Author Contributions: Conceptualization, M.S.S.D.; writing—original draft preparation, M.S.S.D. and L.L.E.-P.; writing—review and editing, M.S.S.D., L.L.E.-P. and M.L.G.; data curation M.S.S.D., L.L.E.-P., I.M.A., M.L.G. and A.M.; supervision, T.S. All authors have read and agreed to the published version of the manuscript.

Funding: This research received no external funding.

Institutional Review Board Statement: Not applicable.

Informed Consent Statement: Not applicable.

Data Availability Statement: Not applicable.

Conflicts of Interest: The authors declare no conflict of interest.

References

1. Shume, W.M.; Murthy, H.C.A.; Zereffa, E.A. A Review on Synthesis and Characterization of Ag_2O Nanoparticles for Photocatalytic Applications. *J. Chem.* **2020**, *2020*, 5039479. [CrossRef]
2. Khin, M.M.; Nair, A.S.; Babu, V.J.; Murugan, R.; Ramakrishna, S. A review on nanomaterials for environmental remediation. *Energy Environ. Sci.* **2012**, *5*, 8075–8109. [CrossRef]
3. Danish, M.S.S.; Estrella, L.L.; Alemaida, I.M.A.; Lisin, A.; Moiseev, N.; Ahmadi, M.; Nazari, M.; Wali, M.; Zaheb, H.; Senjyu, T. Photocatalytic Applications of Metal Oxides for Sustainable Environmental Remediation. *Metals* **2021**, *11*, 80. [CrossRef]
4. Hua, M.; Zhang, S.; Pan, B.; Zhang, W.; Lv, L.; Zhang, Q. Heavy metal removal from water/wastewater by nanosized metal oxides: A review. *J. Hazard. Mater.* **2012**, *211–212*, 317–331. [CrossRef] [PubMed]

5. Schwanke, A.J.; Balzer, R.; Pergher, S. Microporous and Mesoporous Materials from Natural and Inexpensive Sources. In *Handbook of Ecomaterials*; Torres Martínez, L.M., Kharisova, O.V., Kharisov, B.I., Eds.; Springer: Cham, Switzerland, 2019; Volume 136, pp. 3379–3399. [CrossRef]
6. Bi, J.; Wang, J.; Huang, X.; Tao, Q.; Chen, M.; Wang, T.; Hao, H. Enhanced removal of Pb(II) and organics by titanate in a designed simultaneous process. *Sep. Purif. Technol.* **2020**, *251*, 117339. [CrossRef]
7. Nair, G.M.; Sajini, T.; Mathew, B. Advanced green approaches for metal and metal oxide nanoparticles synthesis and their environmental applications. *Talanta Open* **2022**, *5*, 100080. [CrossRef]
8. Danish, M.S.S.; Bhattacharya, A.; Stepanova, D.; Mikhaylov, A.; Grilli, M.L.; Khosravy, M.; Senjyu, T. A Systematic Review of Metal Oxide Applications for Energy and Environmental Sustainability. *Metals* **2020**, *10*, 1604. [CrossRef]
9. Allahverdiyev, A.M.; Abamor, E.S.; Bagirova, M.; Rafailovich, M. Antimicrobial effects of TiO_2 and Ag_2O nanoparticles against drug-resistant bacteria and *leishmania* parasites. *Future Microbiol.* **2011**, *6*, 933–940. [CrossRef]
10. Torabi, S.; Mansoorkhani, M.J.K.; Majedi, A.; Motevalli, S. REVIEW: Synthesis, Medical and Photocatalyst Applications of Nano-Ag_2O. *J. Coord. Chem.* **2020**, *73*, 1861–1880. [CrossRef]
11. Huang, K.; Li, C.; Zheng, Y.; Wang, L.; Wang, W.; Meng, X. Recent advances on silver-based photocatalysis: Photocorrosion inhibition, visible-light responsivity enhancement, and charges separation acceleration. *Sep. Purif. Technol.* **2022**, *283*, 120194. [CrossRef]
12. Wang, X.; Li, S.; Yu, H.; Yu, J.; Liu, S. Ag_2O as a New Visible-Light Photocatalyst: Self-Stability and High Photocatalytic Activity. *Chem.-A Eur. J.* **2011**, *17*, 7777–7780. [CrossRef] [PubMed]
13. Castillo-Henríquez, L.; Alfaro-Aguilar, K.; Ugalde-Álvarez, J.; Vega-Fernandez, L.; Montes de Oca-Vasquez, G.; Vega-Baudrit, J.R. Green Synthesis of Gold and Silver Nanoparticles from Plant Extracts and Their Possible Applications as Antimicrobial Agents in the Agricultural Area. *Nanomaterials* **2020**, *10*, 1763. [CrossRef] [PubMed]
14. Gour, A.; Jain, N.K. Advances in green synthesis of nanoparticles. *Artif. Cells Nanomed. Biotechnol.* **2019**, *47*, 844–851. [CrossRef] [PubMed]
15. Adil, S.F.; Assal, M.E.; Khan, M.; Al-Warthan, A.; Siddiqui, M.R.H.; Liz-Marzán, L.M. Biogenic synthesis of metallic nanoparticles and prospects toward green chemistry. *Dalton Trans.* **2015**, *44*, 9709–9717. [CrossRef]
16. Zhang, D.; Ma, X.-L.; Gu, Y.; Huang, H.; Zhang, G.-W. Green Synthesis of Metallic Nanoparticles and Their Potential Applications to Treat Cancer. *Front. Chem.* **2020**, *8*, 799. [CrossRef]
17. Bouafia, A.; Laouini, S.E.; Tedjani, M.L.; Ali, G.A.; Barhoum, A. Green biosynthesis and physicochemical characterization of Fe_3O_4 nanoparticles using *Punica granatum* L. fruit peel extract for optoelectronic applications. *Text. Res. J.* **2021**. [CrossRef]
18. Dharmaraj, D.; Krishnamoorthy, M.; Rajendran, K.; Karuppiah, K.; Annamalai, J.; Durairaj, K.R.; Santhiyagu, P.; Ethiraj, K. Antibacterial and cytotoxicity activities of biosynthesized silver oxide (Ag_2O) nanoparticles using *Bacillus paramycoides*. *J. Drug Deliv. Sci. Technol.* **2021**, *61*, 102111. [CrossRef]
19. Islam, S.N.; Naqvi, S.M.A.; Parveen, S.; Ahmad, A. Application of mycogenic silver/silver oxide nanoparticles in electrochemical glucose sensing; alongside their catalytic and antimicrobial activity. *3 Biotech* **2021**, *11*, 342. [CrossRef]
20. Elemike, E.E.; Onwudiwe, D.C.; Ekennia, A.C.; Sonde, C.U.; Ehiri, R.C. Green Synthesis of Ag/Ag_2O Nanoparticles Using Aqueous Leaf Extract of *Eupatorium odoratum* and Its Antimicrobial and Mosquito Larvicidal Activities. *Molecules* **2017**, *22*, 674. [CrossRef]
21. El Shafey, A.M. Green synthesis of metal and metal oxide nanoparticles from plant leaf extracts and their applications: A review. *Green Process. Synth.* **2020**, *9*, 304–339. [CrossRef]
22. Ali, A.; Ahmed, T.; Wu, W.; Hossain, A.; Hafeez, R.; Islam Masum, M.; Wang, Y.; An, Q.; Sun, G.; Li, B. Advancements in Plant and Microbe-Based Synthesis of Metallic Nanoparticles and Their Antimicrobial Activity against Plant Pathogens. *Nanomaterials* **2020**, *10*, 1146. [CrossRef] [PubMed]
23. Iravani, S. Green synthesis of metal nanoparticles using plants. *Green Chem.* **2011**, *13*, 2638–2650. [CrossRef]
24. Li, R.; Chen, Z.; Ren, N.; Wang, Y.; Wang, Y.; Yu, F. Biosynthesis of silver oxide nanoparticles and their photocatalytic and antimicrobial activity evaluation for wound healing applications in nursing care. *J. Photochem. Photobiol. B Biol.* **2019**, *199*, 111593. [CrossRef]
25. Ghotekar, S.; Dabhane, H.; Pansambal, S.; Oza, R.; Tambade, P.; Medhane, V. A Review on Biomimetic Synthesis of Ag_2O Nanoparticles using Plant Extract, Characterization and its Recent Applications. *Ad. J. Chem. B* **2020**, *2*, 102–111. [CrossRef]
26. Bouafia, A.; Laouini, S.E.; Ahmed, A.S.A.; Soldatov, A.V.; Algarni, H.; Chong, K.F.; Ali, G.A.M. The Recent Progress on Silver Nanoparticles: Synthesis and Electronic Applications. *Nanomaterials* **2021**, *11*, 2318. [CrossRef] [PubMed]
27. Khan, M.; Shaik, M.R.; Adil, S.F.; Khan, S.T.; Al-Warthan, A.; Siddiqui, M.R.H.; Tahir, M.N.; Tremel, W. Plant extracts as green reductants for the synthesis of silver nanoparticles: Lessons from chemical synthesis. *Dalton Trans.* **2018**, *47*, 11988–12010. [CrossRef]
28. Şuţan, N.A.; Fierăscu, I.; Şuţan, C.; Soare, L.C.; Neblea, A.M.; Somoghi, R.; Fierăscu, R.C. In vitro mitodepressive activity of phytofabricated silver oxide nanoparticles (Ag_2O-NPs) by leaves extract of *Helleborus odorus Waldst. & Kit. ex Willd*. *Mater. Lett.* **2021**, *286*, 129194. [CrossRef]
29. Archana; Sharma, S.N.; Srivastava, R. Silver oxide nanoparticles synthesized by green method from *Artocarpus heterophyllus* for antibacterial and antimicrobial applications. *Mater. Today Proc.* **2020**, *28*, 332–336. [CrossRef]

30. Ravichandran, S.; Paluri, V.; Kumar, G.; Loganathan, K.; Kokati Venkata, B.R. A novel approach for the biosynthesis of silver oxide nanoparticles using aqueous leaf extract of *Callistemon lanceolatus* (Myrtaceae) and their therapeutic potential. *J. Exp. Nanosci.* **2016**, *11*, 445–458. [CrossRef]
31. Rashmi, B.N.; Harlapur, S.F.; Avinash, B.; Ravikumar, C.R.; Nagaswarupa, H.P.; Anil Kumar, M.R.; Gurushantha, K.; Santosh, M.S. Facile green synthesis of silver oxide nanoparticles and their electrochemical, photocatalytic and biological studies. *Inorg. Chem. Commun.* **2020**, *111*, 107580. [CrossRef]
32. Ashokraja, C.; Sakar, M.; Balakumar, S. A perspective on the hemolytic activity of chemical and green-synthesized silver and silver oxide nanoparticles. *Mater. Res. Express* **2017**, *4*, 105406. [CrossRef]
33. Muthukumar, H.; Palanirajan, S.K.; Shanmugam, M.K.; Arivalagan, P.; Gummadi, S.N. Photocatalytic degradation of caffeine and *E. coli* inactivation using silver oxide nanoparticles obtained by a facile green co-reduction method. *Clean Technol. Environ. Policy* **2021**, *24*, 1087–1098. [CrossRef]
34. Shah, A.; Haq, S.; Rehman, W.; Waseem, M.; Shoukat, S.; Rehman, M.-U. Photocatalytic and antibacterial activities of *Paeonia emodi* mediated silver oxide nanoparticles. *Mater. Res. Express* **2019**, *6*, 045045. [CrossRef]
35. Suresh, S.; Pradheesh, G.; Ramani, V.A. Biosynthesis and characterization of CuO, MgO and Ag_2O nanoparticles, anti inflammatory activity and phytochemical screening of the ethanolic extract of the medicinal plant *Pavetta indica* Linn. *J. Pharmacogn. Phytochem.* **2018**, *7*, 1984–1990.
36. Manikandan, V.; Yi, P.-I.; Velmurugan, P.; Jayanthi, P.; Hong, S.C.; Suh, J.M.; Sivakumar, S. Production, optimization and characterization of silver oxide nanoparticles using *Artocarpus heterophyllus* rind extract and their antifungal activity. *Afr. J. Biotechnol.* **2017**, *16*, 1819–1825. [CrossRef]
37. Fayyadh, A.A.; Alzubaidy, M.H.J. Green-synthesis of Ag_2O nanoparticles for antimicrobial assays. *J. Mech. Behav. Mater.* **2021**, *30*, 228–236. [CrossRef]
38. Pradheesh, G.; Suresh, S.; Suresh, J.; Alexramani, V. Antimicrobial and Anticancer Activity Studies on Green Synthesized Silver Oxide Nanoparticles from the Medicinal Plant *Cyathea nilgiriensis Holttum*. *Int. J. Pharm. Investig.* **2020**, *10*, 146–150. [CrossRef]
39. Haq, S.; Yasin, K.A.; Rehman, W.; Waseem, M.; Ahmed, M.N.; Shahzad, M.I.; Shahzad, N.; Shah, A.; Rehman, M.U.; Khan, B. Green Synthesis of Silver Oxide Nanostructures and Investigation of Their Synergistic Effect with Moxifloxacin Against Selected Microorganisms. *J. Inorg. Organomet. Polym. Mater.* **2021**, *31*, 1134–1142. [CrossRef]
40. Abbasi, B.A.; Iqbal, J.; Nasir, J.A.; Zahra, S.A.; Shahbaz, A.; Uddin, S.; Hameed, S.; Gul, F.; Kanwal, S.; Mahmood, T. Environmentally friendly green approach for the fabrication of silver oxide nanoparticles: Characterization and diverse biomedical applications. *Microsc. Res. Tech.* **2020**, *83*, 1308–1320. [CrossRef]
41. Kokila, N.R.; Mahesh, B.; Roopa, K.P.; Prasad, B.D.; Raj, K.; Manjula, S.N.; Mruthunjaya, K.; Ramu, R. *Thunbergia mysorensis* mediated nano silver oxide for enhanced antibacterial, antioxidant, anticancer potential and in vitro hemolysis evaluation. *J. Mol. Struct.* **2022**, *1255*, 132455. [CrossRef]
42. Aiswariya, K.S.; Jose, V. Bioactive Molecules Coated Silver Oxide Nanoparticle Synthesis from *Curcuma zanthorrhiza* and HR-LCMS Monitored Validation of Its Photocatalytic Potency Towards Malachite Green Degradation. *J. Clust. Sci.* **2021**, *32*, 1–12. [CrossRef]
43. Maheshwaran, G.; Bharathi, A.N.; Selvi, M.M.; Kumar, M.K.; Kumar, R.M.; Sudhahar, S. Green synthesis of Silver oxide nanoparticles using *Zephyranthes rosea* flower extract and evaluation of biological activities. *J. Environ. Chem. Eng.* **2020**, *8*, 104137. [CrossRef]
44. Manikandan, V.; Velmurugan, P.; Park, J.-H.; Chang, W.-S.; Park, Y.-J.; Jayanthi, P.; Cho, M.; Oh, B.-T. Green synthesis of silver oxide nanoparticles and its antibacterial activity against dental pathogens. *3 Biotech* **2017**, *7*, 72. [CrossRef] [PubMed]
45. El-Ghmari, B.; Farah, H.; Ech-Chahad, A. A New Approach for the Green Biosynthesis of Silver Oxide Nanoparticles Ag_2O, Characterization and Catalytic Application. *Bull. Chem. React. Eng. Catal.* **2021**, *16*, 651–660. [CrossRef]
46. Armani, M.A.; Abu-Taleb, A.; Remalli, N.; Abdullah, M.; Srikanth, V.V.S.S.; Labhasetwar, N.K. Dragon's blood-aided synthesis of Ag/Ag_2O core/shell nanostructures and Ag/Ag_2O decked multi-layered graphene for efficient As(III) uptake from water and antibacterial activity. *RSC Adv.* **2016**, *6*, 44145–44153. [CrossRef]
47. Laouini, S.; Bouafia, A.; Soldatov, A.; Algarni, H.; Tedjani, M.; Ali, G.; Barhoum, A. Green Synthesized of Ag/Ag_2O Nanoparticles Using Aqueous Leaves Extracts of *Phoenix dactylifera* L. and Their Azo Dye Photodegradation. *Membranes* **2021**, *11*, 468. [CrossRef]
48. Zia, J.; Riaz, U. Microwave-Assisted Degradation of Paracetamol Drug using Polythiophene-Sensitized $Ag–Ag_2O$ Heterogeneous Photocatalyst Derived from Plant Extract. *ACS Omega* **2020**, *5*, 16386–16394. [CrossRef]
49. Sharma, A.; Sharma, S.; Sharma, K.; Chetri, S.P.K.; Vashishtha, A.; Singh, P.; Kumar, R.; Rathi, B.; Agrawal, V. Algae as crucial organisms in advancing nanotechnology: A systematic review. *J. Appl. Phycol.* **2016**, *28*, 1759–1774. [CrossRef]
50. Bakir, E.M.; Younis, N.S.; Mohamed, M.E.; El Semary, N.A. Cyanobacteria as Nanogold Factories: Chemical and Anti-Myocardial Infarction Properties of Gold Nanoparticles Synthesized by *Lyngbya majuscula*. *Mar. Drugs* **2018**, *16*, 217. [CrossRef]
51. Asimuddin, M.; Shaik, M.R.; Fathima, N.; Afreen, M.S.; Adil, S.F.; Siddiqui, M.R.H.; Jamil, K.; Khan, M. Study of Antibacterial Properties of *Ziziphus mauritiana* based Green Synthesized Silver Nanoparticles against Various Bacterial Strains. *Sustainability* **2020**, *12*, 1484. [CrossRef]
52. Dhoondia, Z.H.; Chakraborty, H. *Lactobacillus* Mediated Synthesis of Silver Oxide Nanoparticles. *Nanomater. Nanotechnol.* **2012**, *2*, 15. [CrossRef]

53. Karunagaran, V.; Rajendran, K.; Sen, S. Optimization of Biosynthesis of Silver Oxide Nanoparticles and Its Anticancer Activity. *Int. J. Nanosci.* **2017**, *16*, 05n06. [CrossRef]
54. El-Sheekh, M.M.; Hassan, L.H.; Morsi, H.H. Assessment of the in vitro anticancer activities of cyanobacteria mediated silver oxide and gold nanoparticles in human colon CaCo-2 and cervical HeLa cells. *Environ. Nanotechnol. Monit. Manag.* **2021**, *16*, 100556. [CrossRef]
55. Yildirim, O.; Tunay, D.; Ozkaya, B.; Demir, A. Effect of Green synthesized silver oxide nanoparticle on biological hydrogen production. *Int. J. Hydrogen Energy* **2021**, in press. [CrossRef]
56. Iqbal, S.; Fakhar-E-Alam, M.; Akbar, F.; Shafiq, M.; Atif, M.; Amin, N.; Ismail, M.; Hanif, A.; Farooq, W.A. Application of silver oxide nanoparticles for the treatment of cancer. *J. Mol. Struct.* **2019**, *1189*, 203–209. [CrossRef]
57. Savun-Hekimoğlu, B.; Eren, Z.; Ince, N. Photocatalytic Destruction of Caffeine on Sepiolite-Supported TiO_2 Nanocomposite. *Sustainability* **2020**, *12*, 10314. [CrossRef]
58. Hsin, Y.-H.; Chen, C.-F.; Huang, S.; Shih, T.-S.; Lai, P.-S.; Chueh, P.J. The apoptotic effect of nanosilver is mediated by a ROS- and JNK-dependent mechanism involving the mitochondrial pathway in NIH3T3 cells. *Toxicol. Lett.* **2008**, *179*, 130–139. [CrossRef]
59. Xia, T.; Kovochich, M.; Brant, J.; Hotze, M.; Sempf, J.; Oberley, T.; Sioutas, C.; Yeh, J.I.; Wiesner, M.R.; Nel, A.E. Comparison of the Abilities of Ambient and Manufactured Nanoparticles to Induce Cellular Toxicity according to an Oxidative Stress Paradigm. *Nano Lett.* **2006**, *6*, 1794–1807. [CrossRef]
60. Sambhy, V.; MacBride, M.M.; Peterson, B.R.; Sen, A. Silver Bromide Nanoparticle/Polymer Composites: Dual Action Tunable Antimicrobial Materials. *J. Am. Chem. Soc.* **2006**, *128*, 9798–9808. [CrossRef]
61. Gollapudi, V.R.; Mallavarapu, U.; Seetha, J.; Akepogu, P.; Amara, V.R.; Natarajan, H.; Anumakonda, V. In situ generation of silver and silver oxide nanoparticles on cotton fabrics using *Tinospora cordifolia* as bio reductant. *SN Appl. Sci.* **2020**, *2*, 508. [CrossRef]
62. Hu, Z.; Zhang, J.; Chan, W.L.; Szeto, Y.S. Suspension of Silver Oxide Nanoparticles in Chitosan Solution and its Antibacterial Activity in Cotton Fabrics. *MRS Online Proc. Libr.* **2006**, *920*, 203. [CrossRef]
63. Gouda, M. Nano-zirconium oxide and nano-silver oxide/cotton gauze fabrics for antimicrobial and wound healing acceleration. *J. Ind. Text.* **2012**, *41*, 222–240. [CrossRef]